ACS APPLIED MATERIALS & INTERFACES

Research Article

www.acsami.org

High Performance of Transferring Lithium Ion for Polyacrylonitrile-Interpenetrating Crosslinked Polyoxyethylene Network as Gel Polymer Electrolyte

Ping-Lin Kuo,* Ching-An Wu, Chung-Yu Lu, Chin-Hao Tsao, Chun-Han Hsu, and Sheng-Shu Hou*

Department of Chemical Engineering, National Cheng Kung University, Tainan, 70101, Taiwan, ROC

Supporting Information

ABSTRACT: A polyacrylonitrile (PAN)-interpenetrating cross-linked polyoxyethylene (PEO) network (named XANE) was synthesized acting as separator and as gel polymer electrolytes simultaneously. SEM images show that the surface of the XANE membrane is nonporous, comparing to the surface of the commercial separator to be porous. This property results in excellent electrolyte uptake amount (425 wt %), and electrolyte retention for XANE membrane, significantly higher than that of commercial separator (200 wt %). The DSC result indicates that the PEO crystallinity is deteriorated by the cross-linked process and was further degraded by the interpenetration of the PAN. The XANE membrane shows significantly higher ionic conductivity (1.06−8.21 mS cm^{-1}) than that of the commercial Celgard M824 separator (0.45−0.90 mS cm^{-1}) ascribed to the high electrolyte retention ability of XANE (from TGA), the deteriorated PEO crystallinity (from DSC) and the good compatibility between XANE and electrode (from measuring the interfacial-resistance). For battery application, under all charge/discharge rates (from 0.1 to 3 C), the specific half-cell capacities of the cell composed of the XANE membrane are all higher than those of the aforementioned commercial separator. More specifically, the cell composed of the XANE membrane has excellent cycling stability, that is, the half-cell composed of the XANE membrane still exhibited more than 97% columbic efficiency after 100 cycles at 1 C. The above-mentioned advantageous properties and performances of the XANE membrane allow it to act as both an ionic conductor as well as a separator, so as to work as separator-free gel polymer electrolytes.

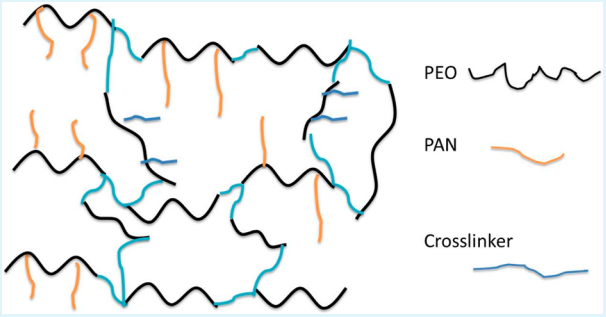

KEYWORDS: *lithium-ion battery, electrolyte, separator-free, polyoxyethylene, polyacrylonitrile*

INTRODUCTION

Recently, lithium-ion batteries with high performance and safety have been considered an attractive power source for a wide variety of applications, such as energy storage systems and electric vehicles.[1−4] However, large capacity batteries require higher safety precautions because of the existence of highly flammable organic liquid electrolytes, which raise the possibility of explosions.[5−9] Gel polymer electrolytes, which feature the characteristics of both solid and liquid electrolytes, have received increasing attention due to wide electrochemical window, and high ionic conductivity, good compatibility with the electrode and high thermal stability.[10−16] However, the application of gel polymer electrolytes in large-scale systems is currently limited because of low stability, poor mechanical strength and high cost.[17−19]

Polyoxyethylene (PEO) is the most commonly used host polymer for preparing gel polymer electrolytes, however, the resulting polymers lose mechanical strength as plasticized by organic solvents. Thus, it is always coated on polypropylene (PP) separator as supporter to obtain mechanical strength. Here, this porous PP film only provides holes to adapt electrolytes solution but cannot adsorb electrolytes solution to transfer Li-ion itself. On the other hand, polyacrylonitrile (PAN) has been used as an alternatively gel polymer electrolytes due to its superior electrical and mechanical properties.[20−22]

In this work, we prepared a composite of PAN interpenetrating cross-linked-PEO, denoted as XANE, where the cross-linking network was further interpenetrated by the high-modulus PAN to constitute a strong skeleton to work as a supporter or separator. This composite itself also can adsorb, uptake/retain a great amount of electrolytes solution (1.0 M $LiPF_6$ in ethylene carbonate (EC)/dimethyl carbonate (DMC)/diethyl carbonate (DEC) (1:1:1 in wt%,)) to transfer lithium ion through PEO segment and PAN segment. The results show that XANE features high ionic conductivity, good mechanical properties, a stable electrochemical window and good thermal stability. The ionic conductivities of the XANE membrane in the temperature range of 25−80 °C are all higher than that of the commercial separator, Celgard M824, because of the high electrolyte retention ability of this membrane. Unlike usual liquid

Received: September 27, 2013
Accepted: February 12, 2014
Published: February 12, 2014

   dx.doi.org/10.1021/am404248b | ACS Appl. Mater. Interfaces 2014, 6, 3156−3162

electrolytes which are impossible to assemble without a conventional separator in a cell, the XANE membrane can be conveniently assembled without a separator in a lithium-ion battery. Under all charge/discharge rates (from 0.1 to 3 C), the specific cell capacities of the cell composed of the XANE membrane are all higher than those of the aforementioned commercial separator. More specifically, in the cycling stability test, the cell composed of the XANE membrane exhibited more than 97% columbic efficiency after 100 cycles at 1 C.

EXPERIMENTAL SECTION

Preparation of XANE Membrane. First, the synthesis of the PEO-b-PAN copolymer was carried out in an aqueous medium. The polyetheramine (Jeffamine ED Series, XTJ-502) and acrylonitrile monomer (Sigma-Aldrich) were placed in the flask. The ceric ammonium nitrate in 1.0 M nitric acid was then added dropwise to the reaction mixture, and polymerization was allowed to proceed with stirring for 6 h. The precipitated polymer was purified first with water to remove the reactant and dry at room temperature in a vacuum for 48 h. The block copolymers thus synthesized were dissolved in dimethylformamide and reprecipitated with methanol.

Then, the polyetheramine and PEO-b-PAN copolymer were mixing under the AN/EO molar ratio = 0, 0.25, 0.35 0.5, 0.65, and 0.75, which donated as XE, XANE25, XANE35, XANE50, XANE65, and XANE75, respectively, followed by the addition of poly(ethylene glycol) diglycidyl ether (PEGDE) (Kyoeisha Chemical Co., Ltd.) under vigorous stirring for 6 h. Then the mixture was cured at 80 °C for 12 h to obtain the membranes. Finally, the films were soaked in organic electrolyte solution, 1.0 M $LiPF_6$ in EC/DMC/DEC (1:1:1 in wt%), from Ubiq Technology Co., Ltd.) over 12 h in an argon-filled glovebox to obtain gel polymer electrolyte for further measurement.

Methods of Characterization. The morphology of the membrane was investigated using a field emission scanning electron microscope (JEOL, JSM-6380LV). IR spectra were obtained with a Nicolet Magna II 550 spectrometer. The ^1H NMR spectra of the monomers and polymers were recorded on a Bruker AMX500 spectrometer using tetramethylsilane (TMS) as an internal standard in $CDCl_3$. A weight loss temperature value was determined by therogravimetric analysis (TGA7, Perkin Elemer) at a heating rate of 20 °C min^{-1} under a nitrogen atomosphere. Differential scanning calorimetry (DSC) measurements were carried out using a TA Instruments Q100 DSC.

Electrochemical Measurements. The ionic conductivity of the gel polymer electrolytes were determined by electrochemical impedance spectroscopy on electrochemical instrument (CHI604A, CH Instrument, Inc.) using alternative current signal with potential amplitude of 10 mV and frequencies from 100 kHz to 10 Hz. In the determination of the ionic conductivity, the gel polymer electrolytes were sandwiched between two parallel stainless steel discs (diameter Φ = 16 mm) of coin cell type. The ionic conductivity was calculated from the bulk electrolyte resistance (R) according to

$$\sigma = l/RS$$

where l is the thickness of the gel polymer electrolytes and S is the contact area between electrolytes and stainless steel discs. The bulk electrolyte resistance (R) was obtained from the complex impedance diagram. The electrochemical stability window of the gel polymer electrolytes were determined by linear sweep voltammetry using a stainless steel working electrode and lithium foil as the counter electrode at the scanning rate of 5 mV s^{-1}. The cathodes of the test cells were prepared by slurry coating a mixture of 80 wt % $LiFePO_4$ powder (Aleees Advanced Lithium Electrochemistry Co., Ltd., Taiwan), 10 wt % Super P, 10 wt % polyvinylidene fluoride (PVDF), and N-methyl-2-pyrrolidone (NMP) onto high purity aluminum foil which was then dried at 100 °C for 24 h in vacuum and pressed. The anode used was high purity lithium metal. The test cells were assembled in a dry, oxygen free glovebox. Charge−discharge testing was performed galvanostatically between 2.5−4.2 V at room temperature on a Battery Automation Test Systems (Acu Tech Systems, BAT-750B).

RESULT AND DISCUSSIONS

Preparation and Characterization of XANE. The XANE membrane was fabricated by cross-linking polyetheramine and PEO-b-PAN copolymer with PEGDE. Supporting Information Figure S1 shows the IR spectra of the purified PEO-b-PAN copolymer, polyetheramine, and PAN. The peak at 2850 cm^{-1} was the result of the CH_2 stretching vibration of EO chain of polyetheramine. The bands at 1450 and 1349 cm^{-1} were due to CH_2 scissoring and wagging vibration of the polymer. The strong peaks at 1100 and 2250 cm^{-1}, respectively, corresponding to the (C−O−C) stretching vibration of polyetheramine and (−CN stretching vibration) PAN, confirm the formation of a PEO-*b*-PAN copolymer.[23] Further, from the ^1H NMR spectrum (Supporting Information Figure S2), the chemical shift values at 2.08 ($-CH_2$) and 3.15 ppm (−CH) for polyetheramine and 3.53 ppm ($-CH_2CH_2O-$) for polyetheramine also confirm the existence of PEO-b-PAN copolymer.[24]

Heat Stability and Electrochemical Stability. The thermal stability is an important property for electrolytes composed of polymers and lithium salts during application in lithium-ion batteries. After cross-linking the mixture of polyetheramine and PEO-b-PAN copolymer by PEGDE, the as-prepared XE, XANE25, XANE35, XANE50, XANE65 and XANE75 membranes showed a 97%, 85%, 84%, 79%, 73%, and 68% weight loss, respectively, between 350 °C (onset) and 600 °C in the TGA curves (Figure 1). Thus, formation of a cross-linked polymer network of the XANE leads to an electrolyte with higher thermal stability. Furthermore, the process of the preparing XANE membrane is very simple and costs of the required raw materials are low.

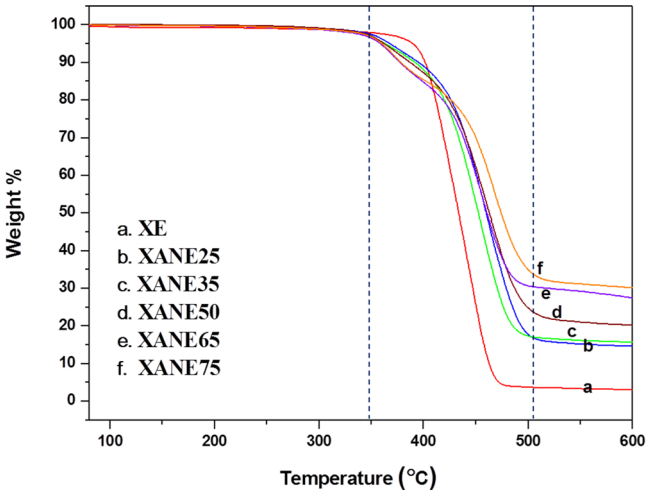

Figure 1. TGA curves of XANE, XE membranes, and commercial separator.

The electrochemical stability of the energy storage device provides essential information for assessing the success. The voltage stability was test by linear sweep voltammetry under the scanning range between 2.0−6.0 V as shown in Figure 2. The LSV curve of XE membrane with the onset oxidation voltage at 4.8 V, while XANE25−XANE75 oxidation reaction potential of about 5.5 V. The result shows that add PAN can increase the stability of XANE membrane because the PAN can induce chemical stability structure through the strong interaction provided by nitrile (−C≡N) group. The onset oxidation voltage of the commercial separator is about 5.2 V. By LSV test,

dx.doi.org/10.1021/am404248b | ACS Appl. Mater. Interfaces 2014, 6, 3156−3162

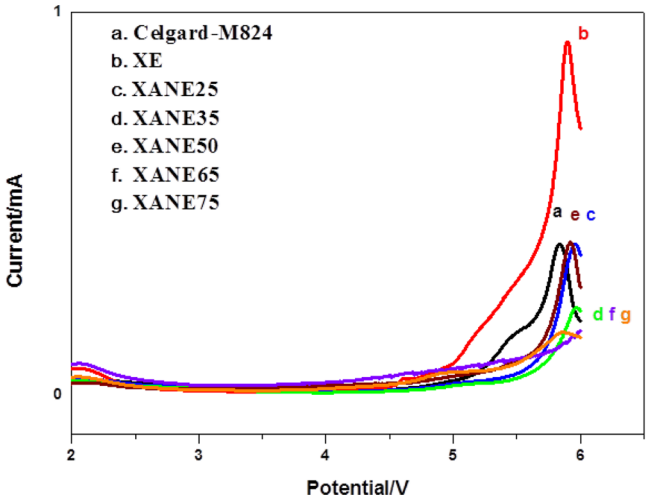

Figure 2. Electrochemical windows for XANE, XE membranes, and commercial separator.

the results show XANE gel electrolyte has good oxidation stability in the 2.0−5.0 V operating voltage environment which is an important issue of battery performance.

Morphology and Corresponding Electrolyte Uptake and Retention. Figure 3a and b displays the SEM images of the

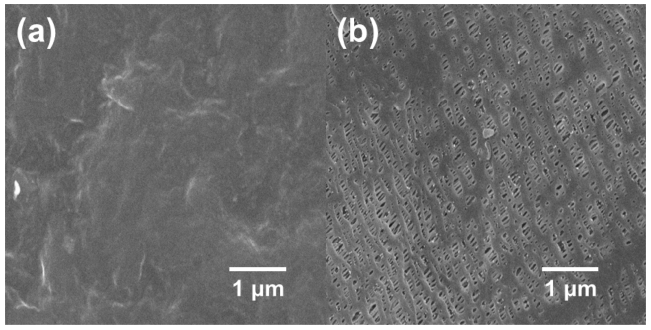

Figure 3. SEM images of (a) XANE membrane and (b) commercial separator.

typical XANE membrane and commercial separator, respectively. It can be seen from Figure 3a that the surface of the XANE membrane is nonporous, which is a highly desirable characteristic since electrolyte retention is crucial to the safety of lithium-ion battery. In comparison, the surface of the commercial separator with pore diameter range from 50 to 200 nm.

This property results in excellent electrolyte retention, that is, the uptake amount of the XE, XANE25, XANE35, XANE50, XANE65, and XANE75 membrane can respectively reach 540, 425, 405, 345, 310, and 295 wt %, which is significantly higher than that of commercial separator (200 wt %). This induce that the ionic conductivity, which is closely related to the amount of organic electrolyte, to higher than the commercial separator. Meanwhile, the TGA curves for equal weights of XANE membrane and commercial separator soaked with the same amount of electrolyte where measured as shown in Figure 4. The emission of large amounts of combustible gases at temperatures below 120 °C is the primary reason for lithium-ion battery accidents such as fires and explosions.[25] However, evaporation of organic gases for XANE membrane is much slower than that for the commercial separator. This property of very slow emission of organic gases and greatly improves the safety of lithium-ion

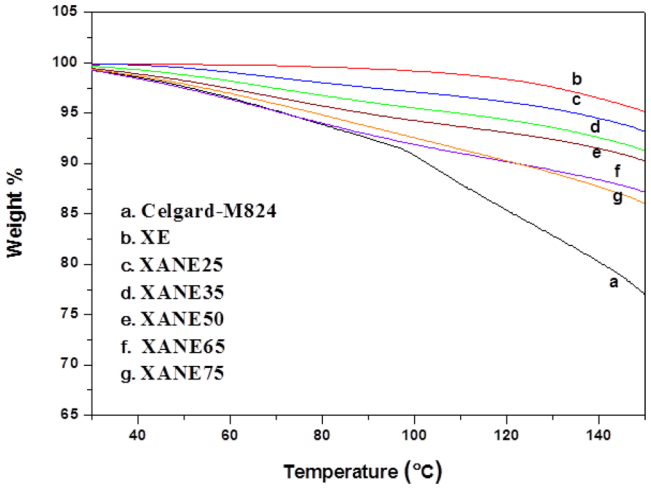

Figure 4. TGA curves of XANE, XE membranes, and commercial separator.

battery. In addition, the proposed membrane also endows lithium-ion battery with good electrochemical performance is mainly contributed by the superior electrolyte retention ability of XANE at high temperature.

PEO Crystallinity Affected by PAN. The effect of interpenetrating PAN on the crystallinity of PEO was investigated through the thermal properties of the polymer membranes using DSC (Figure 5). Melting enthalpy (ΔH) is the

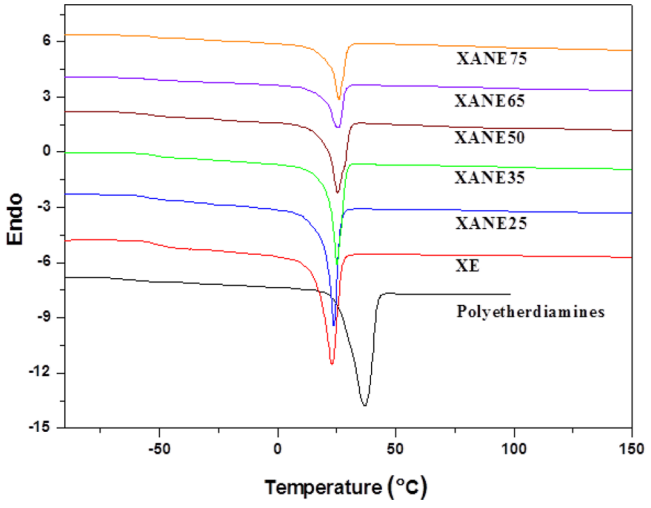

Figure 5. DSC curves of polyetheramines, XE, and XANE membranes.

heat of fusion for the electrolytes which can be calculated from the integral area of the baseline and of each melting curve. The baseline can be designated by connecting two points at which the instant value of its derivative curve becomes zero near melting temperature (T_m). The data of ΔH and Tm, evaluated during the heating process from −90 to 150 °C, are all summarized in Table 1. From the DSC curves, the ΔH of EO ($-CH_2CH_2O-$) for polyetheramine and XE membrane are 151.5 and 100.8 J/g EO, respectively. This implies that the PEO crystallinity deteriorated due to the cross-linked process. Moreover, the ΔH of EO for XE, XANE25, XANE35, XANE50, XANE65, and XANE75 membrane are 100.8, 88.1, 84.2, 83.3, 78.6, and 77.7 J/g EO, respectively, shown that the PEO crystallinity was further degraded by the interpenetration of the PAN.

dx.doi.org/10.1021/am404248b | ACS Appl. Mater. Interfaces 2014, 6, 3156−3162

Table 1. T_g, T_m, ΔH, Electrolyte Uptake Amount, and Specific Discharge Capacies of the Cell Composed of the Polyetherdiamines, XANE, XE Membrane, and Commercial Separator

sample name	T_g (°C)	T_m (°C)	ΔH (J/g EO)	electrolytes uptake amount (wt %)	0.1 C (mAh g^{-1})	1 C (mAh g^{-1})	3 C (mAh g^{-1})
polyetherdiamines	−57.0	36.0	151.5	X	X	X	X
XE	−46.0	23.0	100.8	540	148	111	3
XANE25	−44.0	23.8	88.1	425	153	141	80
XANE35	−42.4	25.2	84.2	405	160	142	90
XANE50	−41.6	25.5	83.3	345	161	149	99
XANE65	−41.3	25.7	78.6	310	150	139	98
XANE75	−40.8	25.9	77.7	295	151	138	100
Celgard-M824	X	X	X	200	154	143	82

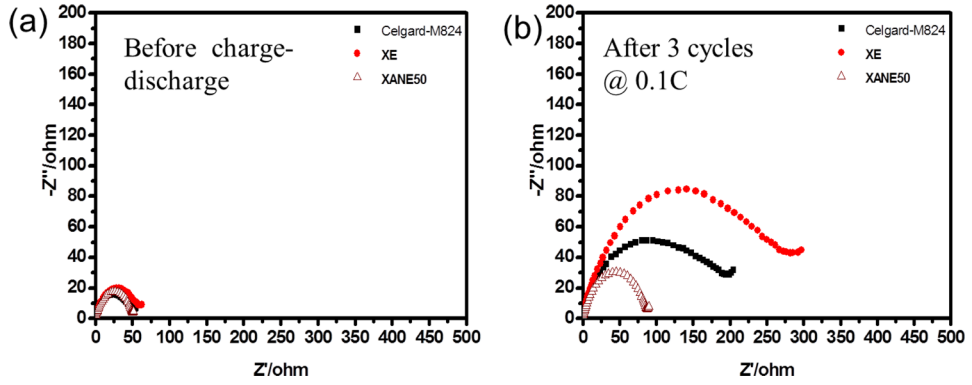

Figure 6. AC-impedance spectra with respect to cycle numbers for XANE50, XE membrane, and commercial separator cells: (a) before charge−discharge and (b) after 3 cycles charge−discharge at 0.1 C.

Compatibility between XANE Membrane and Electrode. Meanwhile, the interfacial compatibility (Figure 6) between the electrolyte and the lithium metal electrode was further characterized through the interfacial resistance between the electrode and the XANE50 membrane measured by using AC-impedance spectroscopy in a coin cell. The AC-impedance response comprised a distorted semicircle at the high frequency region followed by a small spike, both of which are attributed to the presence of a diffusion process. Before charge−discharge cycling, the magnitudes of the interfacial resistances of the cell composed with XANE50, XE membrane, and commercial separator were fairly similar (~50 ohm). However, after 3 charge−discharge cycles at 0.1 C, the resistance value of the commercial separator cell (190 ohm) was nearly double that of the XANE50 membrane cell (85 ohm). In addition, the resistance value of the XE membrane was rapidly increased to 275 ohm. Thus, we can conclude that the XANE50 membrane does not produce a marked increase in electrolyte−electrode interface resistance after charge−discharge cycling because of the better compatibility between the electrode and XANE membrane.[26−28]

Conductivity, Specific Conductivity, and Long-Term Stability. High ionic conductivity and a wide electrochemical window are key requisites for electrolytes intended to battery application. Figure 7 shows the ionic conductivity dependence with respect to temperature for all the XANE membrane and commercial separator saturated with organic electrolyte in the temperature range of 25−80 °C. At 25 °C, the ionic conductivity of the XE, XANE25−XANE75 membrane are 5.0 mS cm^{-1} and ranged from 3.0 and 1.0 mS cm^{-1}, respectively. In addition, for higher temperature (80 °C), the ionic conductivity of the XE, XANE25−XANE75 membrane are 9.0 mS cm^{-1} and ranged from 8.0 and 4.0 mS cm^{-1}, respectively. The result shows that ionic conductivity increasing as the temperature rose due to the

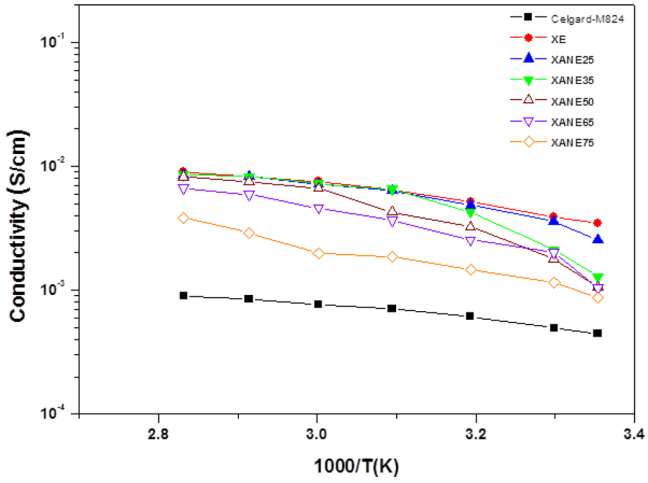

Figure 7. Ionic conductivity versus temperature plots for XANE, XE membranes, and commercial separator.

easier polymer chain movement under high temperature. Furthermore, the ionic conductivities of XE and XANE membranes are higher than that of commercial separator (at 25 and 80 °C, the values are 0.45 and 0.90 mS cm^{-1}, respectively). The results imply that the ionic conductivities of the XANE membranes from 25 to 80 °C are all significantly higher than that of the commercial separator. From above-mentioned results, the high conductivities of XANE can be contributed by: (1) high electrolyte retention ability of XANE as well high electrolytes uptake amount (Figure 4, TGA), (2) deteriorted PEO crystallinity (Figure 5, DSC), and (3) good compatibility between XANE membrane and electrode (Figures 6 and 7, impendence and conductivity measurement).

dx.doi.org/10.1021/am404248b | ACS Appl. Mater. Interfaces 2014, 6, 3156−3162

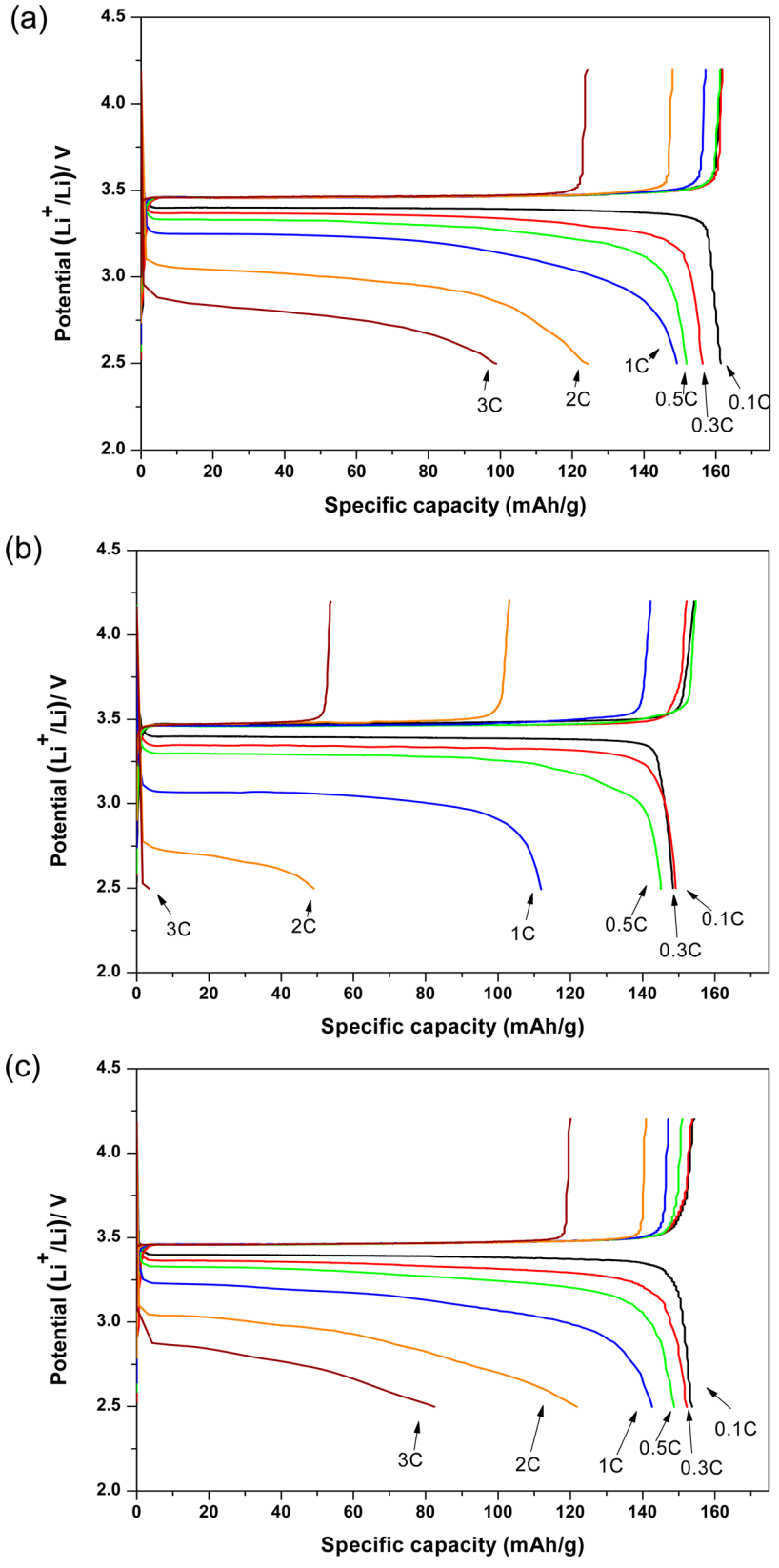

Figure 8. Charge−discharge curves of cells with (a) XANE50, (b) XE membrane, and (c) commercial separator as electrolyte.

The charge−discharge curves of coin cells composed with the XANE50, XE membrane and commercial separator are shown in Figure 8a−c, respectively, and the specific discharge capacities of the cell composed of the XE, all XANE membranes and commercial separator are summarized in Table 1. The cell specific capacities of the coin cells composed with XANE50, XE membrane and commercial separator are respectively 160, 148, and 152 mAh g^{-1} at 0.1 C, while at 3 C, they are 100, 3, and 85

dx.doi.org/10.1021/am404248b | ACS Appl. Mater. Interfaces 2014, 6, 3156−3162

mAh g^{-1}. In $LiFePO_4$ half-cell system, under the charge−discharge procedure, the curve can be seen having a flat platform because of the Fe^{2+}/Fe^{3+} oxidation−reduction reaction, however, in higher charge−discharge rate, the discharge curve starts to decrease earlier because the poor conductivity of the material caused by the polarization. The result shows that cells composed of the cross-linked polymer without PAN (XE) has poor performance at 3 C, it means the existence of PAN in a cross-linked polymer network of the XANE membrane leads to an electrolyte with higher mechanical stability which improve the rate performance. Moreover, the capacitor of cells composed with XANE50 is higher than that of Celgard-M824, especially in higher C rate, possibly because of higher electrolyte adsorption of XANE50 membrane.

For long-term stability test, the cells made with XANE 50 membrane and commercial separator were tested under charge at 0.1 C and discharge at 1 C discharge for 100 charge−discharge cycles as shown in Figure 9. The cell made with XANE50

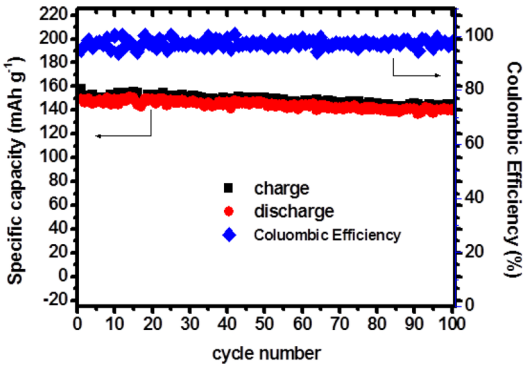

Figure 9. Cycling performances of cells with XANE50 membrane as separator.

membrane had first discharge capacitor of 149 mAh g^{-1}, after 100 cycle charge−discharge cycles, there are still capacitance value of 140 mAh g^{-1}, and the columbic efficiency values was close to 97%, which means that a very low level of capacitance values recession. The result shows that the cell composed with XANE50 membrane has excellent reversible charge−discharge cycle performance and battery stability.

CONCLUSIONS

The surface of the XANE membrane is nonporous, results in excellent electrolyte retention of commercial separator, low emission of combustible gases below 120 °C. This property of very slow emission of organic gases greatly improves the safety of lithium ion battery at high temperature. The high ionic conductivities of the XANE membrane can be contributed by: (1) high electrolyte retention ability of XANE as well high electrolytes uptake amount, (2) deteriorated PEO crystallinity, and (3) good compatibility between XANE membrane and electrode. The existence of PAN in XANE membrane leads to an electrolyte with higher mechanical stability which improves the rate performance. The cell made of XANE50 membrane has excellent reversible charge−discharge cycle performance and battery stability with first discharge of 149 mAh g^{-1}, after 100 cycle charge−discharge cycles, there are still capacitance value of 140 mAh g^{-1}, and the columbic efficiency values is close to 97%.

ASSOCIATED CONTENT

Supporting Information

FT-IR and ^1H NMR data. This material is available free of charge via the Internet at http://pubs.acs.org.

AUTHOR INFORMATION

Corresponding Authors

*Tel.: +886-6-275 7575. Fax: +886-6-276 2331. E-mail: plkuo@mail.ncku.edu.tw.

*E-mail: sshou@mail.ncku.edu.tw.

Notes

The authors declare no competing financial interest.

ACKNOWLEDGMENTS

The authors would like to thank the National Science Council, Taipei, ROC, for their generous financial support of this research.

REFERENCES

(1) Croce, F.; Appetecchi, G. B.; Persi, L.; Scrosati, B. *Nature* **1998**, *394*, 456−458.
(2) Armand, M.; Tarascon, J. M. *Nature* **2008**, *451*, 652−657.
(3) Venugopal, G.; Moore, J.; Howard, J.; Pendalwar, S. *J. Power Sources* **1999**, *77*, 34−41.
(4) Chu, P. P.; Reddy, M. J. *J. Power Sources* **2003**, *115*, 288−294.
(5) Lee, Y. S.; Lee, J. H.; Choi, J. A.; Yoon, W. Y.; Kim, D. W. *Adv. Funct. Mater* **2013**, *23*, 1019−1027.
(6) Ju, S. H.; Lee, Y. S.; Sun, Y. K.; Kim, D. W. *J. Mater. Chem. A* **2013**, *1*, 395−401.
(7) Wu, F.; Tan, G.; Chen, R.; Li, L.; Xiang, J.; Zheng, Y. *Adv. Mater.* **2011**, *23*, 5081−5085.
(8) Croce, F.; Focarete, M. L.; Hassoun, J.; Meschini, I.; Scrosati, B. *Energy Environ. Sci.* **2011**, *4*, 921−927.
(9) Patel, M.; Gnanavel, M.; Bhattacharyya, A. J. *J. Mater. Chem.* **2011**, *21*, 17419−17427.
(10) Wang, S. H.; Hou, S. S.; Kuo, P. L.; Teng, S. H. *ACS Appl. Mater. Interfaces* **2013**, *5*, 8477−8485.
(11) Varshney, P. K.; Gupta, S. *Ionics* **2011**, *17*, 479−483.
(12) Fergus, J. W. *J. Power Sources* **2010**, *195*, 4554−4569.
(13) Christie, A. M.; Lilley, S. J.; Staunton, E.; Andreev, Y. G.; Bruce, P. *Nature* **2005**, *433*, 50−53.
(14) Carol, P.; Ramakrishnan, P.; John, B.; Cheruvally, G. *J. Power Sources* **2011**, *196*, 10156−10162.
(15) Egashira, M.; Todo, H.; Yoshimoto, N.; Morita, M. *J. Power Sources* **2008**, *178*, 729−735.
(16) Stephan, A. M. *Eur. Polym. J.* **2006**, *42*, 21−42.
(17) Fu, D.; Luan, B.; Argue, S.; Bureau, M. N.; Davidson, I. J. *J. Power Sources* **2012**, *206*, 325−333.
(18) Cho, T. H.; Tanaka, M.; Ohnishi, H.; Kondo, Y.; Yoshikazu, M.; Nakamura, T.; Sakai, T. *J. Power Sources* **2010**, *195*, 4272−4277.
(19) Rao, M. M.; Liu, J. S.; Li, W. S.; Liao, Y. H.; Liang, Y.; Zhao, L. Z. *J. Solid State Electrochem.* **2010**, *14*, 255−261.
(20) Koken, N.; Karagoz, S.; Kizilcan, N.; Ustamehmetoglu, B. *J. Appl. Polym. Sci.* **2013**, *127*, 3790−3797.
(21) Watanabe, M.; Kanba, M.; Nagaoka, K.; Shinohara, I. *J. Appl. Polym. Sci.* **1982**, *27*, 4191−4198.
(22) Abraham, K. M.; Alamgir, M. *J. Electrochem. Soc.* **1990**, *137*, 1657−1658.
(23) Huang, J.; Huang, X.; Hu, W.; Lou, W. *J. Polym. Sci., Part A: Polym. Chem.* **1998**, *34*, 1317−1324.
(24) Huang, C. H.; Wu, C. A.; Hou, S. S.; Kuo, P. L.; Hsieh, C. T.; Teng, H. S. *Adv. Funct. Mater.* **2012**, *22*, 4677−4685.
(25) Zhu, Y.; Wang, F.; Liu, L.; Xiao, S.; Chang, Z.; Wu, Y. *Energy Environ. Sci.* **2013**, *6*, 618−624.
(26) Cao, J.; Wang, L.; He, X.; Fang, M.; Gao, J.; Li, J.; Deng, L.; Chen, H.; Tian, G.; Wang, J.; Fan, S. *J. Mater. Chem. A* **2013**, *1*, 5955−5961.

(27) Saikia, D.; Wu, H. Y.; Pan, Y. C.; Lin, C. P.; Huang, K. P.; Chen, K. N.; Fey, G. T. K.; Kao, H. M. *J. Power Sources* **2011**, *196*, 2826−2834.
(28) Song, J. Y.; Wang, Y. Y.; Wan, C. C. *J. Power Sources* **1999**, *77*, 183−197.